Particle Accelerators
1978, Vol. 8, pp. 211–216

RESONANT INSTABILITIES IN THE COAXIAL AUTOACCELERATOR

JOHN G. SIAMBIS

Plasma Physics Division, Naval Research Laboratory, Washington, D.C. 20375 USA

(Received May 19, 1977; in final form November 11, 1977)

The resonance and stability conditions of the traveling-wave type longitudinal bunching mode and transverse beam breakup mode of thin solid and thin hollow intense relativistic electron beams inside several autoaccelerator systems have been examined by means of a coupled-mode approach. For the case of the iris-loaded cylindrical waveguide system, which behaves as a slow wave structure, we find that the beam slow waves couple to the autoaccelerator fundamental modes and instability results in agreement with existing experimental results and other theoretical predictions. For the case of the coaxial cavity autoaccelerator, which does not behave as a slow wave structure, we find that the beam slow waves only couple to very high spatial harmonics of the autoaccelerator propagating modes, thereby leading to stability againt the resonant instabilities in this case.

I. INTRODUCTION

Linear accelerators are most often long cylindrical pipes with accelerating elements inserted or attached periodically to the cylindrical pipe. When the spacing and the geometry of the accelerating elements remain invariant along the length of the cylindrical pipe then a periodic structure is obtained. Examples of linear periodic accelerators are the following. The linear induction accelerator as realized in the Astron Injector.[1,2] The traveling wave (rf) accelerators as realized in the Stanford Linear Accelerator (SLAC).[3] The autoaccelerator as realized in the iris-loaded waveguide structures at the Lebedev Institute[4] and the Lawrence Livermore Laboratory[5] and the coaxial cavity structure at the Naval Research Laboratory[6–8] and elsewhere.[9,10]

The stability of electron and ion beams accelerated by these periodic structures to high energies is a very important design constraint particularly when a high current is desired as well.[2] The instabilities that occur in the beam flow in these periodic structures have been traditionally divided into two types of interactions[11]: the nonresonant interactions, such as virtual cathode phenomena and instabilities, klystron instability, resistive wall and inductive wall instabilities and the resonant interactions,[2] such as the traveling-wave type longitudinal bunching mode (TM_{01} mode) and transverse beam breakup mode (TM_{11} mode). In this work we have called the traveling-wave type interactions resonant interactions, because a *local* resonance condition, between the slow negative energy waves on the beam and the waves supported by the accelerator structure has to be satisfied locally along the length of the system. To be sure, some of the interactions referred to in this work as nonresonant contain a *global* resonance condition, which comes about in order to maximize the interaction, as is the case with the klystron instability.[17]

In this paper we shall examine the resonant instabilities of beam flow by means of a coupling of modes method.[12] That is the dispersion characteristics of the linear periodic accelerating structure are established in the absence of the beam (Section II). Next the beam dispersion characteristics are established for a uniform cylindrical pipe in the absence of the periodic accelerating elements (Section III). Then the intersection of the two uncoupled dispersion characteristics yields the real frequency and wavelength for the resonant interaction, Section IV. The growth rate or *e*-folding length of the instability can also be obtained by reconsidering the coupled system in the neighborhood of the coupling resonance.[16]

This method permits an easy and graphical representation of the resonant instability properties of various accelerator configurations and facilitates comparison of various geometries and beam parameters. More specifically this method has been used in this work to predict that the coaxial

cavity autoaccelerator[6,7,9] is stable against resonant instabilities. In addition this method has also been used here to provide independent confirmation of the long wavelength resonant instabilities that have been predicted and observed experimentally in the iris-loaded waveguide autoaccelerator.[5] This method also permits placing in evidence the physical mechanisms that are responsible for a stable configuration in the former case and an unstable configuration in the latter case.

II DISPERSION CHARACTERISTICS OF ACCELERATING STRUCTURES

In general there are two types of accelerating elements for linear accelerators, those that are placed inside the circular waveguide, that is like an iris-loaded waveguide, Figure 1a, and those that are placed outside the circular waveguide, that is cavities connected through gaps to the accelerator, Figures 1b and 1c.

The iris loaded waveguide, appropriate for modeling one version of the autoaccelerator and the rf linear accelerator, has been extensively studied. Approximate dispersion relations for the lowest passbands of the TM_{01} and TM_{11} modes are given[3] respectively by

$$\omega \simeq \omega_{01} + \Omega_{01}(1 - \cos kl_o) \tag{1}$$

$$\omega \simeq \omega_{11} + \Omega_{11}(1 - \cos kl_o), \tag{2}$$

where l_o is the length of a section, ω_{01} and ω_{11} are the cutoff frequencies for the TM_{01} and TM_{11} modes respectively and Ω_{01} and Ω_{11} are the respective half-bandwidths. The cutoff frequencies are given by

$$\omega_{01} = \frac{c\zeta_{01}}{r_o} \tag{3}$$

$$\omega_{11} = \frac{c\zeta_{11}}{r_o}, \tag{4}$$

where c is the velocity of light and r_o the radius of the waveguide and ζ_{mn} is the nth root of the mth order Bessel function $J_m(\zeta_{mn}) = 0$ appropriate for the mode under consideration. The two values needed here are $\zeta_{01} = 2\pi/2.6$ and $\zeta_{11} = 2\pi/1.64$. The half bandwidth Ω can be calculated through a laborious analytical procedure[13] or preferably by relating it to experimentally measurable quantities.[3]

The dispersion relations for the geometries shown in Figures 1b and 1c are difficult to obtain and in general are not available. What can be established easily, however, is the cutoff frequency for the TM_{01} and TM_{11} modes propagating in the waveguide in the absence of the gaps. When the gap length is much smaller than the gap spacing, $l_g \ll l_o$, then the lowest passband dispersion relations for the respective modes will be given by Eqs. (1) and (2). Inspection of Figures 1b and 1c shows that the coupling from section to section in the axial direction, in both of these cases, is capacitive, because of the longer path that the current in the waveguide walls has to follow due to the presence of the gaps. This observation allows to conclude that the dispersion relation for both cases will be of the form given in Eqs. (1) and (2). That is the lowest passband will lie above the cutoff frequency, as opposed to inductive coupling, from section to section in the axial direction, where the lowest passband lies below the cutoff frequency as shown in Figures 1.7 and 1.8 of Ref. 14. The half-bandwidths Ω_{01} and Ω_{11} will depend on the gap lengths l_g/l_o and the geometrical and electromagnetic details of the external cavities, and their exact values are not needed in this work. The passbands of Eqs. (1) and (2) consist of spatial harmonics in k-space with periodicity $k_o = 2\pi/l_o$, which is the

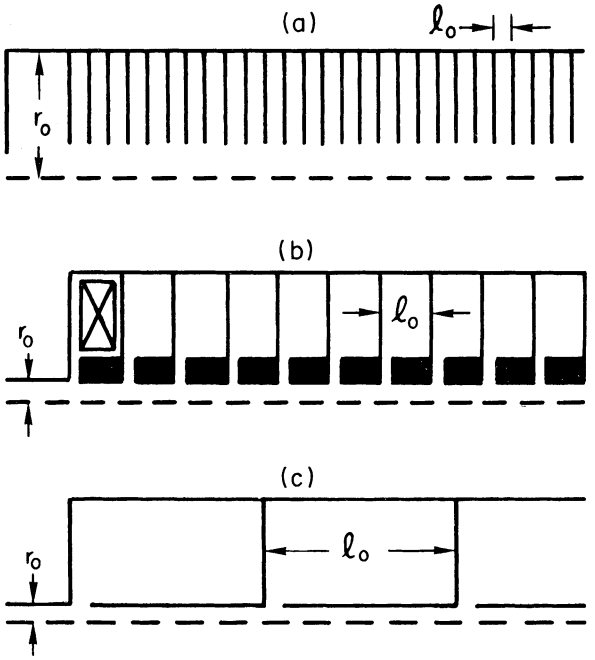

FIGURE 1 Comparative schematic diagrams of linear periodic accelerators; (a): the iris-loaded waveguide; (b): the linear-induction accelerator; (c) the coaxial autoaccelerator.

width of the fundamental period. When power is fed in the periodic structure at a frequency ω within the passband many of the spatial harmonics are excited in order to satisfy the boundary conditions but the amplitude of the higher order spatial harmonics decreases as $1/n^2$, where n is the order of the spatial harmonic.[13] Also note that the ratio of the lower cutoff frequencies for the two passbands of interest here is

$$\frac{\omega_{11}}{\omega_{01}} = \frac{\zeta_{11}}{\zeta_{01}} \simeq 1.6. \tag{5}$$

III DISPERSION CHARACTERISTICS OF BEAMS

For the applications of interest here we consider thin intense relativistic electron beams situated on the axis, $r_b \ll r_o$, or of thin annular shape $\Delta r_b \ll r_b \lesssim r_o$ situated near the wall of the drift tube. For the case of the beam longitudinal bunching mode we utilize well known asymptotic expressions for the dispersion relation in the limits of small and large k. For the case of the transverse beam breakup mode we derive the corresponding asymptotic forms of the dispersion relation.

For the beam longitudinal bunching mode and for the limit $kr_o < 1$, the dispersion relation as given by Briggs,[15] is

$$1 - \frac{(k^2c^2 - \omega^2)\alpha}{(\omega - kU_b)^2} = 0, \tag{6}$$

where U_b is the velocity of the beam and α is given by

$$\alpha = \frac{I}{\beta\gamma^3 I_o} \tag{7}$$

where

$$\beta = \frac{U_b}{c}; \qquad \gamma^2 = (1 - \beta^2)^{-1} \tag{8}$$

$$I_o = \frac{2\pi\varepsilon_o m_o c^2}{q_e \ln(r_o/r_b)} = \frac{8.5}{\ln(r_o/r_b)}, \quad \text{in kA}, \tag{9}$$

where I is the beam current, ε_o is the vacuum permittivity, m_o and q_e are the electron rest mass and charge respectively and r_b is the radius of the beam, both for thin solid beams on-axis and thin hollow beams off-axis. The slow-wave branch of Eq. (6) is given by

$$\frac{\omega}{c} = \left[\frac{\beta - \alpha(1 + (1 - \beta)/\alpha)^{1/2}}{1 + \alpha}\right]k. \tag{10}$$

The high frequency-short wavelength limit of the slow-wave dispersion relation is given by the well-known expression

$$\frac{\omega}{c} + \frac{\omega_{pe}}{c\gamma^{3/2}} = \beta k, \tag{11}$$

where ω_{pe} is the beam rest-mass plasma frequency. Comparison of Eqs. (10) and (11) indicates that Eq. (10) is valid for $k \ll k_m = 2\pi r_o$ and Eq. (11) is valid for $k \gg k_m$. For the intermediate region, $k \approx k_m$, approximate expressions for the dispersion relation can also be constructed from Eqs. (10) and (11) but will not be needed here. Note that the change in γ due to the accelerating or decelerating quasistatic potentials at the gaps has been neglected in both Eqs. (10) and (11).

For the case of the transverse beam breakup mode (TM_{11}-type mode) we need consider only the case of the thin solid beam on the axis of the circular waveguide in the presence of a uniform axial magnetic field B_o. An infinitesimal displacement of the beam in the x-direction is assumed of the form

$$\boldsymbol{\xi} = \hat{\imath}_x \xi_o e^{j(\omega t - \phi - kz)}, \tag{12}$$

which generates an axial surface current on the beam of the form

$$\mathbf{J}_s = \hat{\imath}_z \xi_o J_o e^{j(\omega t - \phi - kz)}, \tag{13}$$

where J_o is the current density of the beam, assumed uniform, and ϕ is the azimuthal coordinate of the cylindrical coordinate system. The magnetic B and electric E fields produced by this surface current are obtained from the vector potential $\mathbf{A}$

$$\mathbf{A} = \hat{\imath}_z R(r) e^{j(\omega t - \phi - kz)} \tag{14}$$

$$\mathbf{B} = \nabla \times \mathbf{A} \tag{15}$$

$$\mathbf{E} \simeq -\frac{\partial \mathbf{A}}{\partial t}. \tag{16}$$

By solving Laplace's equation inside and outside the surface current and by matching boundary conditions at the surface current interface and at the outer conducting pipe boundary the magnetic field inside the beam is found to be

$$\mathbf{B} = \hat{\imath}_y \tfrac{1}{2}\mu_o \xi_o J_o e^{j(\omega t - kz)} \qquad \text{for } k \ll k_m, \tag{17}$$

and

$$\mathbf{B} \to \sqrt{k}e^{-k} \to 0 \qquad \text{for } k \gg k_m. \tag{18}$$

The equation of motion for the displacement ξ in the $\phi = 0$ plane is given by

$$\left(\frac{\partial}{\partial t} + U_b\frac{\partial}{\partial z}\right)\left[\gamma\left(\frac{\partial \xi}{\partial t} + U_b\frac{\partial \xi}{\partial z}\right)\right] = \frac{q_e \mathbf{U}_b \times \mathbf{B}}{m_e}. \tag{19}$$

The dispersion relations in the limits of Eqs. (17) and (18) are next obtained neglecting the variation of γ due to accelerating or decelerating gap potentials.

$$(\omega - kU_b)^2 = (k_t U_b)^2, \qquad k \ll k_m \tag{20}$$

$$\omega = kU_b, \qquad k \gg k_m, \tag{21}$$

where $k_t^2 = \omega_{pe}^2/2\gamma c^2$. In the intermediate region $k \simeq k_m$ approximate values for the dispersion relation will have to be assumed if needed. The slow wave branch of Eq. (20) is given by

$$\omega = (k - k_t)U_b. \tag{22}$$

IV INSTABILITIES

In this section we shall consider the interaction and resonant coupling of the modes obtained in Section II for the accelerating structure and the modes obtained in Section III for the beam. As numerical examples we shall use the iris-loaded waveguide autoaccelerator of Ref. 5 and the coaxial cavity loaded waveguide autoaccelerator of Refs. 6 and 8. Comparison of these two systems will permit some useful and general conclusions to emerge.

The iris structure has the following parameters: $r_o = 0.15$ m, $l_o = 0.027$ m, yielding $\omega_{01}/c = 16$, $\omega_{11}/c = 25.6$, $k_o = 232$, $k_m = 42$. The coaxial structure has the parameters: $r_o = 0.025$ m, $l_o = 1$ m, yielding $\omega_{01}/c = 97$, $\omega_{11}/c = 155$, $k_o = 6.28$, $k_m = 251$. The resulting cutoff frequencies are marked with dashed horizontal lines in Figure 2 for the TM_{01} mode and in Figure 3 for the TM_{11} mode. For the iris structure there is shown just one period, the fundamental, with an assumed bandwidth of $0.6\omega_{01}$ and $0.6\omega_{11}$, consistent with experimental observations. For the coaxial structure there are shown the first period and the tenth, twentieth and thirtieth spatial harmonics, with an assumed bandwidth of $0.3\omega_{01}$ and $0.3\omega_{11}$, consistent with experimental measurements on the structure. The velocity of light line, marked by the number 1.0 and having slope one, shows that the iris structure,

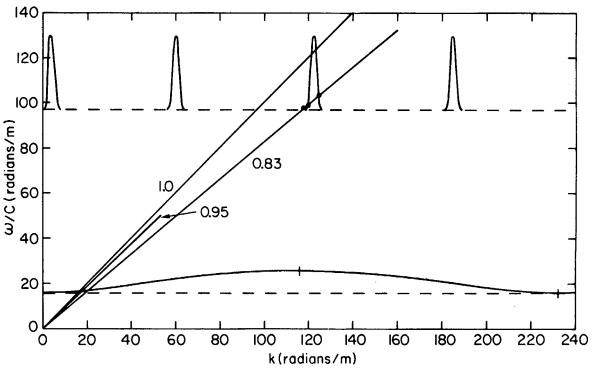

FIGURE 2 Dispersion diagrams and resonance intersections for the longitudinal bunching mode.

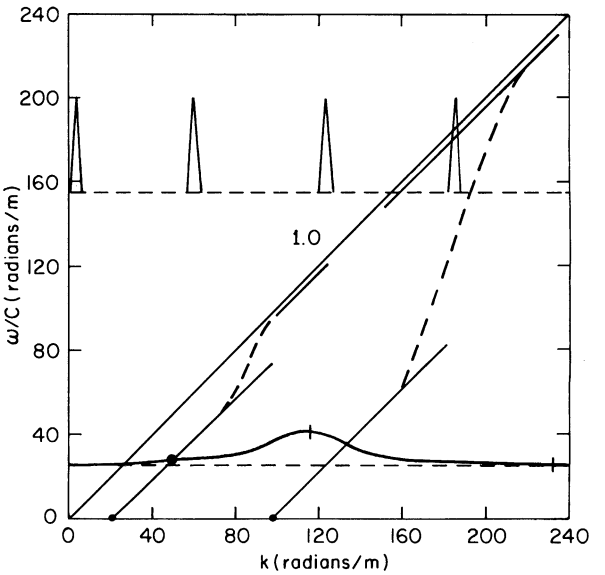

FIGURE 3 Dispersion diagrams and resonance intersections for the transverse beam-breakup mode.

compared to the coaxial structure, is a much more efficient slow-wave generator by virtue of the large width, k_o, of the fundamental period resulting from the close spacing of the periodic accelerating elements and also by virtue of the low cutoff frequency resulting from the larger radius of the pipe. By comparison the coaxial structure produces slow waves only at very high spatial harmonics, i.e., $n \geq 16$ for the TM_{01} mode and $n \geq 25$ for the TM_{11} mode, hence it does not qualify as a slow-wave structure and has never been used as such.

The electron-beam quantities for the iris-structure experiment are as follows. Beam current: 6 kA, $\gamma = 5$, injected $\gamma = \gamma_o = 6.53$, $I_o = 4$ kA, $\beta = 0.98$. These parameters give the following

values for the dispersion relations of Eqs. (10) and (11) respectively:

$$\frac{\omega}{c} = 0.95\,\mathrm{k}, \tag{23}$$

$$\frac{\omega}{c} + 6.0 = 0.98\,\mathrm{k}. \tag{24}$$

The two dispersion curves of Eqs. (23) and (24) intersect at extremely high values of k, $k \gg k_m$, hence the dispersion relation of Eq. (23) is an accurate representation of the beam slow wave dispersion relation in the neighborhood where it intersects the iris structure dispersion relation, Figure 2. This intersection occurs at $\omega = \omega_r = 5.1 \times 10^9$, $k_r = 17$ radians/m which is in excellent agreement with the experimentally observed frequency of, $\omega_r = 5.2 \times 10^9$, for the longitudinal bunching instability. In order to find the e-folding length for this instability, which is convective, the problem must be solved again near the resonance condition, taking into account the coupling. This has been done in Refs. 2 and 16. From Ref. 16 the associated equivalent growth rate ω_I is given by $\omega_I/\omega_r \approx 0.2/\gamma$. The resonance condition for the transverse beam breakup mode is next obtained for the iris structure, from Eqs. (22), (11) and (24) and shown in Figure 3 with $k_t = 21.33$. The low frequency-small k portion of the curve is shown as a solid line. The dashed curve shows the transition to the high frequency-large k asymptotic form of the dispersion relation given by Eq. (21). The resonance condition is obtained at $\omega_r/c \simeq 26$ radians/m and $k_r \simeq 50$ radians/m, which is in excellent agreement with the experimentally observed value of $\omega_r/c \simeq 25$ radians/m. The growth rate for this case has been given in Refs. 5 and 2.

For the case of the coaxial autoaccelerator of Ref. 8 it is not really necessary to pursue the resonant instability question because the slow waves on the beam interact only with the very high spatial harmonics of the periodic structure as shown in Figures 2 and 3. The beam parameters are assumed as follows: peak beam current 40 kA, $\gamma_o = 3$, $r_b = 0.023$ m, $\Delta r_b = 0.003$ m, $I_o = 85$ kA, $\gamma = 2.5$, $\beta = 0.92$. Figure 2 shows the slow-wave beam branch appropriate for the longitudinal bunching instability intersecting the nineteenth, twentieth, and higher spatial harmonics of the periodic structure. These harmonics in order to satisfy boundary conditions on the structure must excite the fundamental and lower spatial harmonics at much higher levels than their own, hence they decay even when driven by the beam. This resonant interaction therefore can only lead to some low-level noise on the beam and not to an instability. A similar conclusion is obtained for the transverse beam breakup mode in Figure 3. For this case we consider only a thin beam on the axis, because the thin hollow beam, far from the axis, would not couple to the transverse beam breakup mode which is operational near the axis of the system. For the thin beam on axis we assume $I = 10$ kA, $\gamma = 5$. $r_b = 0.005$ m, and $\beta = 0.98$, which give $k_t = 98$ radians/m. An approximate transition from the low-frequency to the high-frequency limit is also indicated with a dashed curve.

V CONCLUSIONS

The resonant instabilities for the iris and coaxial autoaccelerators have been considered by making use of the periodicity of the accelerator structures. For the iris structure agreement has been obtained with existing experimental evidence and other theoretical predictions. For the coaxial autoaccelerator stability is predicted against the resonant instabilities because the coaxial structure does not support slow waves that can interact resonantly with the beam except at very high spatial harmonics. The case of the Astron-type accelerator, Figure 1b, can therefore be regarded as an intermediate case between the clearly unstable case of the iris structure,[2] Figure 1a, and the clearly stable case of the coaxial autoaccelerator, Figure 1c, and therefore capable of being tuned to a marginally stable operating point, as has been observed experimentally.[2]

ACKNOWLEDGMENTS

The author acknowledges with pleasure useful discussions with R. Briggs, A. Drobot, M. Friedman, T. Godlove, and V. K. Neil. This work was supported by the Office of Naval Research.

REFERENCES

1. J. W. Beal et al., *IEEE Trans. Nucl. Sci.*, **NS-16**, 294 (1969).
2. V. K. Neil and R. K. Cooper, *Particle Accelerators*, **1**, 111 (1970).
3. R. Helm, Proc. 1966 Linear Accelerator Conf., Los Alamos, p. 254.
4. L. Kazanskii et al., *At. Energ.* **30**, 27 (1971).
5. R. J. Briggs, et al., Ninth Intern. Conf. on High Energy Accelerators, p. 278, 1974.
6. M. Friedman, *Phys. Rev. Lett.* **31**, 1107 (1973).

7. J. Siambis, *Phys. Fluids* **19**, 1784 (1976).
8. J. K. Burton et al., *IEEE Trans. Nucl. Sci.*, **NS-24**, 1628 (1977).
9. V. A. Bashmakov et al., *Zh. Tekh. Fiz.* **43**, 1092 (1973) [*Sov. Phys.-Tech. Phys.* **18**, 696 (1973)].
10. I. A. Grishaev et al., *Zh. Tekh. Fiz.* **44**, 1743 (1974) [*Sov. Phys.-Tech. Phys.* **19**, 1087 (1975)].
11. V. K. Neil, private communication.
12. R. J. Briggs, *Electron Stream Interactions with Plasmas*, (MIT Press, Cambridge, Massachusetts, 1964), p. 39.
13. R. G. E. Hutter, *Beam and Wave Electronics in Microwave Tubes* (D. Van Nostrand Co. Inc., Princeton, N.J., 1960), Chapter 7.
14. D. A. Watkins, *Topics in Electromagnetic Theory* (John Wiley and Sons Inc., New York, 1958), Chapter 1.
15. R. J. Briggs, *Phys. Fluids* **19**, 1257 (1976).
16. V. G. Gapanovich and A. N. Lebedev, *Zh. Tekh. Fiz.* **45**, 844 (1975) [*Sov. Phys.-Tech. Phys.* **20**, 532 (1976)].
17. J. G. Siambis and M. Friedman, *Particle Accelerators*, **8**, 217 (1978).